SJÄLVSTÄNDIGA ARBETEN I MATEMATIK

MATEMATISKA INSTITUTIONEN, STOCKHOLMS UNIVERSITET

Berry's Phase for Quantum Graphs

av

Vladislav Shubin

2026 – No M3

Berry's Phase for Quantum Graphs

Vladislav Shubin

Självständigt arbete i matematik 30 högskolepoäng, avancerad nivå

Handledare: Pavel Kurasov

2026

Abstract

In this thesis, we formulate a model of topology change on the metric figure-eight graph via a continuous one-parameter family of vertex conditions. We show that when the parameter θ traverses a closed cycle $[0, 2\pi]$, the eigenfunctions acquire Berry's phase of π. This demonstrates a direct connection between Berry's phase and topology change in quantum graphs.

Sammanfattning

I denna avhandling formulerar vi en modell för topologiförändring på den metriska figur-åtta-grafen via en kontinuerlig enparametrig familj av nodbetingelser. Vi visar att när parametern θ genomlöper en sluten cykel $[0, 2\pi]$, förvärvar egenfunktionerna Berrys fas π. Detta påvisar ett direkt samband mellan Berrys fas och topologiförändring i kvantgrafer.

Acknowledgements

First and foremost, I would like to thank Pavel for his guidance and for introducing me to quantum graphs. His deep knowledge and our discussions played a crucial role in shaping this work.

I am especially thankful to Mina for his valuable feedback on the thesis. Special thanks go to Fabian and Julian for carefully reading the manuscript and providing helpful comments. I would also like to thank Ruben for valuable discussions on quantum graphs and for pointing me to relevant literature.

Finally, I thank my mother for always supporting me during my studies, especially when things got difficult. I also owe thanks to my friend Artem, whose encouragement set me on this path.

This document has been typeset using typst 0.14.2.

Contents

Introduction

Mathematics has often served as both the foundation and the outcome of scientific progress. Nowhere is this symbiotic relationship more evident than in theoretical physics: while physical intuition has frequently guided the evolution of functional analysis, the formulation of physical theories—particularly in quantum mechanics and gauge theories—would have been impossible without the corresponding advancement of mathematical formalism. This connection, famously described by Wigner as the 'unreasonable effectiveness of mathematics' [7], is particularly profound when geometric and topological structures are used to describe physical states.

In the 1950s, Wheeler was one of the first to formulate the idea of *topology change* [24]. The essence of this idea is that any physical model can be viewed as a topological structure that changes over time, where this topological structure is usually considered as some topological manifold with an operator acting on this structure. This is a remarkably powerful language that allows us to glue, rip apart, and bend manifolds as our theory pleases.

In 1995, Balachandran et al. [1] studied topology change associated with a change in the domain of self-adjointness of an operator defined on a relatively simple topological object—two segments with connected endpoints (see Figure 1). This effect is achieved by changing the boundary conditions connecting the endpoints of the segments, which gives a particular type of topology change. That is, a change in the *domain of the operator* rather than a literal tearing of space.

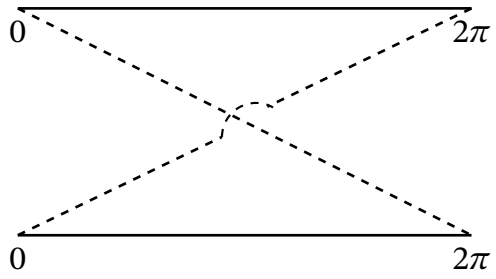

Figure 1: Model of Balachandran [1].

In this sense, Balachandran fundamentally reverses the perspective: now a certain operator and its domain define the topology. A change in boundary conditions leads to a change in topology. Subsequently, Shapere et al. [16] considered a continuous transformation of a similar model based on the theory of quantum graphs. The authors gave many examples of how changes in boundary conditions lead to different geometric

properties and noted the importance of the spectral properties of the operator. Cheon et al. [5], inspired by this model, formulated a slightly different quantum graph with special boundary conditions. As a result, they discovered *quantum holonomy*, which is considered a generalization of the geometric phase [4], [20]. In this thesis, we study a similar system and find *Berry's phase*.

Differential operators can be defined on different topological structures. One such structure has become quite popular in recent decades; we have already mentioned it above. That is the *quantum graph*—a differential operator defined on a graph structure. However, this is not a discrete graph structure, as is usually assumed. Instead, we start with *metric graphs*: in the discrete situation the edges are nothing more than connections between vertices, whereas in the metric case all the edges have lengths. A graph is called *metric* if it consists of intervals of disjoint copies of the real line glued together at the vertices of the graph. This is a dual perspective, where the emphasis shifts from vertices to edges.

Graph models are well-suited for systems where the neighborhood consists of relatively low-dimensional manifolds. Quantum graphs appear when we are interested in describing transport or propagation of waves on a nearly one-dimensional manifold. While the word *quantum* hints at a connection with quantum mechanics, quantum graphs are more than a model of quantum mechanics.

In this thesis, we work with the *figure-eight graph*, consisting of two circles connected at a point, as shown in the following figure:

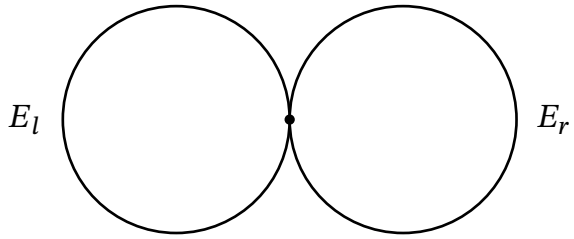

Figure 2: The figure-eight graph model.

The effect of this vertex on the propagation of waves on the graph is the subject of our interest. It is this quantum graph that was used in the aforementioned paper by Cheon et al. [5]. Kurasov and Serio in [11] used this graph to find topological properties generated by vertex conditions. However, the vertex conditions were fixed.

We will use vertex conditions very similar to those in Kurasov [11], varying them continuously with a period of 2π to induce a topology change. In fact, our model

presents a richer topological evolution, causing the eigenfunctions to acquire a non-trivial Berry's phase.

Topology change prior to Balachandran's work, as we have described it, represented a change in the topology of the manifold itself. Matrasulov et al. in [13] considered a quantum star graph (one vertex and n edges), where the length of the edges changed while the vertex conditions remained unchanged—sometimes these models are referred to as driven graphs, i.e. graphs perturbed by time-dependent external forces. This is an example of a classical topology change on a quantum graph. A more general study of such graphs was carried out by Smilansky and Sofer in [17]. The authors also discovered Berry's phase, further demonstrating a connection between Wheeler's topology change and geometric phases in quantum graph models.

Geometric phase was also found on quantum graphs without topology change. Inoue et al. [9] studied Dirac zero modes on a flower graph (a single vertex with n loops) and showed that the resulting Berry connection is non-Abelian, providing a realization of Yang-Mills instanton configurations. This particular work is part of a broader line of research on higher-dimensional fermion models on quantum graphs, initiated by Fujimoto et al. [8].

Contribution

The primary contribution of this thesis is the rigorous formulation of *topology change* on the metric figure-eight graph via a continuous one-parameter family of vertex conditions. While the spectral properties of this graph were previously analyzed by Tibbling [21], this work provides the first explicit construction of a continuous eigenfunction family over a closed parameter loop $\theta \in [0, 2\pi]$. We derive the secular equation for the figure-eight graph under specialized vertex conditions and prove that the Hamiltonian can be deformed smoothly while preserving the spectrum (for equal edge lengths).

We further provide an explicit calculation of the eigenfunction coefficients as a function of the parameter θ, revealing a continuous change that results in a sign-flip ($1 \mapsto -1$). This confirms the existence of *Berry's phase of* π in this model, extending the body of work of Shapere et al. [16] and Cheon et al. [5].

Thesis Structure

The thesis is organized as follows:

- **Chapter 1** provides the mathematical foundations of quantum graphs and geometric phases. In **Section 1.1**, we offer a self-contained introduction to differential operators on graphs, while **Section 1.2** defines the geometric phase in a mathematical context.
- **Chapter 2** defines the figure-eight graph and shows topology change (**Section 2.1**), introduces graph symmetries (**Section 2.2**), and then derives the secular equation (**Section 2.3**).
- **Chapter 3** presents the core result: the existence of Berry's phase on the figure-eight metric graph (**Section 3.1**). In addition, it presents a hypothesis regarding the existence of Berry's phase in a more general situation (**Section 3.2**).

1. Preliminaries

In this chapter, we survey the necessary background on quantum graphs, vertex conditions, and geometric phases. We first introduce the basics of spectral geometry. For a comprehensive introduction, we suggest the reader have a look at some literature by Kurasov [10]. In addition, we suggest a very short introduction by Berkolaiko [2]. In this chapter we follow both Kurasov and Berkolaiko. In this thesis, we assume elementary knowledge of analysis and differential equations.

Next, we give an elementary account of Berry's phase, which is the best-known geometric phase. For a comprehensive overview of these phases, we recommend a book by Bohm et al. on geometric phases in physics [4] or a short introductory paper by Sprinkart et al. [19]. Prior knowledge of quantum mechanics is not required for this thesis, however, in case the reader finds this interesting, we recommend looking at a classical book by Sakurai [15] or a PhD thesis by Katharina Durstberger [6].

1.1. Quantum Graphs

A classical discrete graph is a pair $\Gamma = (V, E)$, where V is a set of vertices $v_1, \ldots, v_N$ and $E \subset V \times V$ is a set of edges—unordered pairs $\{v_i, v_j\}$ for some $i, j = 1, \ldots, N$. We denote N as the number of vertices and M as the number of edges. Also, we define the incidence relation $\sim$ that describes connections. Each edge connects a pair of vertices. We write $e_1 \sim e_2$ for $e_1, e_2 \in E$ if there exists $v \in V$ such that $v \in e_1$ and $v \in e_2$. The notation $v \sim e$ is equivalent to $v \in e$.

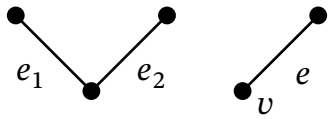

Figure 3: Relations $e_1 \sim e_2$ and $v \sim e$.

For analytical applications we need to make analysis on graphs possible. One way is to formulate classical operators of analysis for discrete graphs. This approach leads to the so-called algebraic spectral geometry of graphs; see Spielman [18] for an introduction. Interestingly, spectral properties of discrete graphs are closely connected to spectral properties of quantum graphs (see Chapter 24 in [10]). The other way leads to metric graphs.

Metric Graphs

A *metric graph* is, informally, a graph whose edges have lengths. To define it we can assign for each edge $e \in E$ a positive length L_e and, thus, identify every such e with an interval $[0, L_e]$ (this is the elementary approach from Berkolaiko [2]). This makes Γ a *metric graph*.

Unfortunately, this approach proves insufficient. Take two edges $e_1 = [0, L_{e_1}]$ and $e_2 = [0, L_{e_2}]$ such that $e_1 \sim e_2$. That means two edges can be joined at zeros: it is not clear which is the 0 on e_1 and which is the 0 on e_2. The same can happen if $L_{e_1} = L_{e_2}$. Thus, we take another approach from Kurasov [10].

In the graph Γ we have M edges; we also assume any vertex is connected by at least one edge. We identify edges e_k with the following:

$$E_k = [x_{2k-1}, x_{2k}], \quad k = 1, 2, \ldots, M,$$

where the x's are endpoints and $x_{2k-1} \leq x_{2k}$. Henceforth, we will treat edges of the graph Γ as intervals E_k. As we identify edges e_k with intervals of real line E_k it is important to note that for *each* k we have a *separate* copy of the real line $\mathbb{R}$, so we do not have an ambiguity of joining intervals as before.

Now we need to restore the set of vertices in this situation. Previously, V contained vertices $v_1, \ldots, v_N$, but metric graphs work with endpoints x_k. Let

$$\boldsymbol{V} = \{x_k\} = \bigcup_{k=1}^{M} \{x_{2k-1}, x_{2k}\}.$$

In this case each vertex v_k becomes an equivalence class V^k of all endpoints at the vertex v_k. Two endpoints are equivalent if either they are the same point on the same edge, or they are both identified with the same vertex.

This leads to a new equivalence relation for the endpoints $x, y \in \mathbb{R}$:

$$x \sim y \Leftrightarrow \begin{bmatrix} \exists E_k : x, y \in E_k \text{ and } x = y, \\ \exists V^k : x, y \in V^k. \end{bmatrix}$$

Now we can define a metric graph in the following way

Definition 1.1 ([10]): Consider M finite closed intervals E_k belonging to *separate* (disjoint) copies of $\mathbb{R}$, called ***edges***, and a partition of the set $\boldsymbol{V}$ of their endpoints into equivalence classes V^k called ***vertices***: $\boldsymbol{V} := \bigcup_{k=1}^{N} V^k$, where N is the number of vertices. The corresponding ***metric graph*** Γ is the union of the edges with the endpoints belonging to the same vertex identified.

This notion can also be seen as the quotient metric space

$$\Gamma = \bigcup_{k=1}^{M} E_k / \sim .$$

A measure can be induced naturally. We work with functions on Γ that form the Hilbert space

$$L_2(\Gamma) = \bigoplus_{k=1}^{N} L_2(x_{2k-1}, x_{2k}).$$

Thus, we also define

$$\int_\Gamma f(x)\,\mathrm{d}x := \sum_{k=1}^{M} \int_{E_k} f(x)\,\mathrm{d}x.$$

Functions in $L_2(\Gamma)$ are not defined point-wise, hence the Hilbert space does not reflect how the edges are connected to each other.

Differential Operators

The differential operator H on the metric graph Γ, broadly speaking, describes the dynamics of waves or particles traveling along the edges. The following differential operators are used in most of the literature:

- the *Laplace* operator

$$H = -\frac{d^2}{dx^2};$$

- the *Schrödinger* operator

$$H_q = -\frac{d^2}{dx^2} + q(x);$$

- the *magnetic Schrödinger* operator

$$H_{q,a} = \left(i\frac{d}{dx} + a(x)\right)^2 + q(x).$$

One can study any other differential operator like the Dirac operator studied by Fujimoto [8], but Schrödinger is the most common.

In the physical picture, the magnetic Schrödinger operator $H_{q,a}$ describes quantum particles moving under the influence of the electric potential q and the magnetic potential a. The case where both magnetic and electric potentials vanish corresponds to free motion and is described by the Laplace operator $H \equiv H_0 \equiv H_{0,0}$.

For the sake of simplicity, we use rather strong assumptions on $q(x)$ and $a(x)$:

- the potentials are real $q(x), a(x) \in \mathbb{R}$;
- the electric potential is essentially bounded $q(x) \in L_\infty(\Gamma)$;
- the magnetic potential is continuously differentiable $a(x) \in C^1(\Gamma \setminus \boldsymbol{V})$.

In this case

$$\mathrm{Dom}\big(H_{q,a}\big) = \big\{f \in L_2(\Gamma) : H_{q,a}f \in L_2(\Gamma)\big\} = W_2^2(\Gamma \setminus \boldsymbol{V}),$$

where W_p^q denotes the Sobolev space.

Indeed, it suffices to observe

$$H_{q,a}f = -f'' + 2iaf' + \big(ia' + a^2\big)f.$$

The function $\big(ia' + a^2\big)f$ belongs to $L_2(\Gamma)$ since a is continuous. It follows that $if' + af \in W_1^2(\Gamma \setminus \boldsymbol{V})$, and hence $f \in W_2^2(\Gamma \setminus \boldsymbol{V})$.

It will be convenient to define values $f(x_k)$ for $x_k \in V^k$ by

$$f(x_k) \coloneqq \lim_{x \to x_k} f(x).$$

Since we work with $f \in W_2^2(\Gamma \setminus \boldsymbol{V})$, this limit exists.

For the function f continuously differentiable on the edges, we define ***normal derivatives*** by

$$\partial f(x_k) \coloneqq \begin{cases} \lim_{x \to x_k} \frac{d}{dx} f(x), & x_k \text{ is the left endpoint,} \\ -\lim_{x \to x_k} \frac{d}{dx} f(x), & x_k \text{ is the right endpoint.} \end{cases}$$

The limits are taken from inside of the corresponding interval. The normal derivatives are independent of the direction in which the edge is parametrised and always point inside the interval.

The *boundary form* of an operator $H_{q,a}$ is the sesquilinear form defined by $\mathcal{B}(f, g) \coloneqq \langle H_{q,a}f, g\rangle - \langle f, H_{q,a}g\rangle$, which measures the failure of symmetry. The

operator is symmetric if and only if $\mathcal{B} \equiv 0$. Thus, to understand the domain where the operator H is symmetric, we need to calculate the boundary form:

$$\begin{aligned}
&\langle H_{q,a} f, g\rangle - \langle f, H_{q,a} g\rangle \\
&= \sum_{n=1}^{M} \Bigg\{ \int_{E_n} \overline{\left[\left(i\frac{d}{dx} + a(x)\right)^2 + q(x)\right] f(x)} \cdot g(x)\,\mathrm{d}x \\
&\quad - \int_{E_n} \overline{f(x)} \cdot \left[\left(i\frac{d}{dx} + a(x)\right)^2 + q(x)\right] g(x)\,\mathrm{d}x \Bigg\}.
\end{aligned}$$

Note that $q(x)$ cancels out. Let $D = \left(\frac{d}{dx} - ia(x)\right)$ so $D^2 = -\left(i\frac{d}{dx} + a(x)\right)^2$, then using integration by parts we get

$$\int_{E_n} Df(x)g(x)\,\mathrm{d}x + \int_{E_n} f(x)\overline{D}g(x)\,\mathrm{d}x = [f(x_k)g(x_k)]_{k=2n-1}^{2n}.$$

Using this fact, we calculate each integral separately:

$$\begin{aligned}
&\int_{E_n} \overline{\left(i\frac{d}{dx} + a(x)\right)^2 f(x)} g(x)\,\mathrm{d}x \\
&\quad = -\int_{E_n} \overline{D^2 f(x)} g(x)\,\mathrm{d}x = -\left[\overline{Df(x_k)} g(x_k)\right]_{k=2n-1}^{2n} + \int_{E_n} \overline{Df(x)} Dg(x)\,\mathrm{d}x.
\end{aligned}$$

$$\begin{aligned}
&\int_{E_n} \overline{f(x)} \cdot \left(i\frac{d}{dx} + a(x)\right)^2 g(x)\,\mathrm{d}x \\
&\quad = -\int_{E_n} \overline{f(x)} D^2 g(x)\,\mathrm{d}x = -\left[\overline{f(x_k)} Dg(x_k)\right]_{k=2n-1}^{2n} + \int_{E_n} \overline{Df(x)} Dg(x)\,\mathrm{d}x.
\end{aligned}$$

Therefore,

$$\begin{aligned}
&\langle H_{q,a}f, g\rangle - \langle f, H_{q,a}g\rangle \\
&= \sum_{n=1}^{M} \Big[\overline{f(x_k)}Dg(x_k)\Big]_{k=2n-1}^{2n} - \Big[\overline{Df(x_k)}g(x_k)\Big]_{k=2n-1}^{2n} = \\
&= \sum_{x_j \in \boldsymbol{V}} \Big\{\overline{\partial f(x_j)}g(x_j) - \overline{f(x_j)}\partial g(x_j)\Big\},
\end{aligned}$$

where we use the notion of ***extended normal derivatives***:

$$\partial f(v) := \begin{cases} \lim_{x\to v}\Big(\frac{d}{dx}f(x) - ia(x)f(x)\Big), & x_j \text{ is the left endpoint,} \\ -\lim_{x\to v}\Big(\frac{d}{dx}f(x) - ia(x)f(x)\Big), & x_j \text{ is the right endpoint.} \end{cases}$$

Thus, the boundary form of the operator $H_{q,a}$ on the metric graph Γ is

$$\begin{aligned}
\mathcal{B}_\Gamma(f, g) &:= \langle H_{q,a}f, g\rangle - \langle f, H_{q,a}g\rangle \\
&= \sum_{x_j \in \boldsymbol{V}} \Big\{\overline{\partial f(x_j)}g(x_j) - \overline{f(x_j)}\partial g(x_j)\Big\}.
\end{aligned} \tag{1}$$

In what follows, we require our operator to be symmetric. Since the boundary form involves only function values at vertices, any set of equations such that $\mathcal{B}_\Gamma \equiv 0$ for some functional space are called ***vertex conditions***.

Definition 1.2: A *quantum graph* is a triple (Γ, H, C), where Γ is a metric graph, H is a Schrödinger operator, and C is a set of vertex conditions. We refer to its spectrum as the *spectrum of the quantum graph*. The standard Laplacian is uniquely determined by the metric graph, therefore if H is a Laplacian we call (Γ, H, C) a metric graph and we refer to its spectrum as the *spectrum of the metric graph*.

Standard Vertex Conditions

We work with self-adjoint differential operators. For that we need to establish the domain of H: that is the purpose of *vertex conditions*. One of the most basic vertex conditions is *the continuity condition*: for any function f on the graph Γ *the continuity condition* is satisfied at the vertex V^k if the following holds:

$$\forall x_i, x_j \in V^k \Rightarrow f(x_i) = f(x_j).$$

Usually in theory and applications one is concerned with the Laplacian operator. It is well known that, for problems of this type, we need additional vertex conditions to define the domain of the operator [10]. The standard condition to use on the derivatives for metric graphs is

$$\sum_{x_j \in V^k} \partial f(x_j) = 0.$$

It is common to call it the *Kirchhoff condition* [2].

We say that the *standard vertex condition* is imposed at the vertex v for a function f if the function satisfies the continuity condition and the Kirchhoff condition at v.

1.1.1. Examples

Trivial Example

Consider an interval $[0, L]$ formed by the point $x_1 = 0$ and $x_2 = L$. That is the simplest metric graph with two vertices $V^1 = \{x_1\}$ and $V^2 = \{x_2\}$; and one edge $E = [0, L]$. Let H be the standard Laplacian. This means that the domain of H is $W_2^2((0, L))$. We impose the standard condition on this graph. The continuity condition does not yield anything since the degree of any vertex is simply 1. On the other hand, the Kirchhoff condition gives

$$0 = \sum_{x_j \in V^1} \frac{df}{dx}(x_j) = \quad f'(0),$$

$$0 = \sum_{x_j \in V^2} \frac{df}{dx}(x_j) = -f'(L).$$

We get a minus in the second equation due to the sign convention for normal derivatives (the normal derivative points to the edge at each endpoint) as shown on the following figure

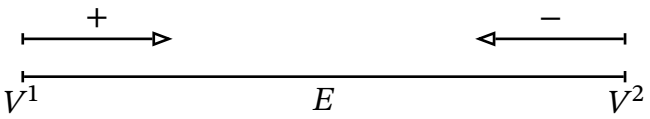

Figure 4: $[0, L]$-graph.

The equation for the eigenvalues $Hf = \lambda f$ becomes

$$-f'' = k^2 f,$$

where $\lambda = k^2$. This is an ordinary differential equation with the solutions

$$f(x) = c_1 \cos kx + c_2 \sin kx.$$

Applying the standard conditions we have

$$c_2 = 0$$

and

$$-c_1 k \sin kL + c_2 k \cos kL = 0.$$

Thus, our eigenfunctions are $f(x) = c_1 \cos\left(\frac{\pi n x}{L}\right)$, for $n \in \mathbb{N}$ and the only eigenvalue we missed is $\lambda = 0$. In this case $f(x) \equiv 1$. Therefore,

$$\mathrm{sp}([0, L]) = \left\{\left(\frac{\pi n}{L}\right)^2 : n = 0, 1, 2, \ldots\right\}.$$

Two Joint Intervals

The situation is less trivial when two intervals are joined. In this case we get the following graph

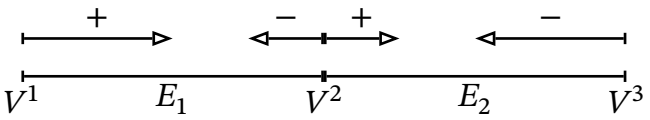

Figure 5: Graph of two intervals.

where $V^1 = \{x_1\}$, $V^2 = \{x_2, x_3\}$, and $V^3 = \{x_4\}$.

In this situation, the only difference from one interval graph happens at vertex V^2, thus let $x_2 = x_3 = L_1$. Now by standard conditions we have $f(x_2) = f(x_3)$ and

$$\sum_{x_j \in V^2} \partial f(x_j) = -f'(L_1) + f'(L_1) = 0.$$

To solve the second order differential equations uniquely, the values $f(L_1)$ and $f'(L_1)$ have to be determined. From the standard condition we have $f(x_2) = f(x_3)$ and $f'(x_2) = f'(x_3)$. Therefore, solutions for the two interval graph are the same as solutions for the interval graph $[0, L_1 + L_2]$, where $x_4 = L_2$. Thus: *a standard vertex of degree* 2 *is equivalent to having an uninterrupted edge* [2].

1.1.2. Vertex Conditions

Now we move to the more general treatment of vertex conditions. Assume we work with an arbitrary quantum graph (Γ, H, C).

Assume v_n is a vertex of degree d_n and V^n is an equivalence class of $\boldsymbol{V}$. Let $\vec{f}(V^n) = \{f(x_j)\}_{x_j \in V^n}$ and $\partial\vec{f}(V^n) = \{\partial f(x_j)\}_{x_j \in V^n}$. A pair $\left(\vec{f}(V^n), \partial\vec{f}(V^n)\right)$ of vectors $\vec{f}(V^n)$ and $\partial\vec{f}(V^n)$ is called ***limit values*** of function f at vertex v. Now we can write the boundary form (1) as follows

$$\mathcal{B}_\Gamma(f, g) = \sum_{n=1}^{N} \langle \partial\vec{f}(V^n), \vec{g}(V^n) \rangle_{\mathbb{C}^{d_n}} - \langle \vec{f}(V^n), \partial\vec{g}(V^n) \rangle_{\mathbb{C}^{d_n}}. \qquad (2)$$

All well-known examples of vertex conditions can be written from (2) as follows:

- Dirichlet conditions:

$$\vec{f}(V^n) = \vec{0},$$

- Neumann conditions:

$$\partial\vec{f}(V^n) = \vec{0},$$

- (generalized) Robin conditions:

$$\partial\vec{f}(V^n) = A\vec{f}(V^n),$$

where A is a Hermitian matrix in $\mathbb{C}^{d_n}$.

However, we can describe a more general construction of vertex conditions. Primarily, we are interested in those conditions that give a self-adjoint operator on the graph. These conditions are called ***Hermitian***.

Definition 1.3: Vertex conditions relating the limit values $\left(\vec{f}, \partial\vec{f}\right) \in \mathbb{C}^{2d}$ at a vertex $v \in V$ of degree d are called *Hermitian* if and only if

- the boundary form $\mathcal{B}_\Gamma$ vanishes whenever f and g satisfy these conditions, and
- the subspace in $\mathbb{C}^{2d}$ formed by all limit values satisfying these conditions has the maximal dimension d.

One can describe d-dimensional subspace $M \subset \mathbb{C}^{2d}$ by the image of a linear map from $\mathbb{C}^d$ to $\mathbb{C}^{2d}$. By considering the subspace

$$M = \left\{U = (B^*t, A^*t) : t \in \mathbb{C}^d\right\},$$

where $A, B \in M_d(\mathbb{C})$. In this fashion one can prove the following theorem.

Theorem 1.4 ([22]): Any Hermitian vertex condition at the vertex v of degree d can be written in the form

$$A\vec{\psi} = B\partial\vec{\psi}. \tag{3}$$

The $d \times d$ matrices A and B can be chosen arbitrarily, provided that the rank of the $d \times 2d$ matrix (A, B) is maximal, and the matrix AB^* is Hermitian.

1.1.3. Scattering Matrix

The scattering matrix is the matrix that describes the change of the wave going through a vertex v. More precisely, if we have an incoming wave $\vec{b} = (b_i)$ to the vertex v, where b_i are the amplitudes, then the reflected wave is $\vec{a} = S_v(k)\vec{b}$. The matrix $S_v(k)$ is called the *vertex scattering matrix* corresponding to the energy $\lambda = k^2$. This matrix is always unitary, but in general depends on the energy.

Consider a vertex v of degree d and its scattering matrix $S_v(k)$. Then we are interested only in the waves around the vertex. In other words, in order to determine $S_v(k)$ we need to consider the local dynamics near the vertex v disregarding the rest of the graph. Thus, any vertex of degree d can be seen as an infinite star graph.

Imagine a vertex of degree 6. Then we have the following graph.

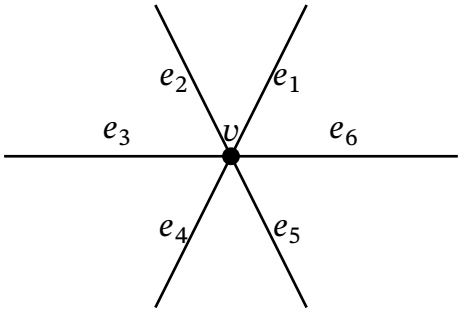

Figure 6: Infinite star graph.

It has one vertex v and six edges $e_s = [0, \infty)$ for $s = 1, \ldots, 6$. Considering the Laplacian on the graph, the general solution takes the form

$$\psi_s(x) = a_s e^{ikx} + b_s e^{-ikx}.$$

Let $\vec{a} = (a_s)_s$ and $\vec{b} = (b_s)_s$. Then $\vec{\psi} = \vec{a} + \vec{b}$ and $\partial\vec{\psi} = -ik\vec{b} + ik\vec{a}$. Substituting $S_v(k)\vec{b} = \vec{a}$ we obtain the following system

$$\begin{cases} \vec{\psi} = \vec{b} + S_v(k)\vec{b}, \\ \partial\vec{\psi} = -ik\vec{b} + ikS_v(k)\vec{b}, \end{cases}$$

where $\left(\vec{\psi}, \partial\vec{\psi}\right)$ form limit values at vertex v, therefore, by Theorem

$$A(I + S_v(k))\vec{b} = Bik(-I + S_v(k))\vec{b},$$

leading to

$$A + ikB = -(A - ikB)S_v(k).$$

We obtain

$$S_v(k) = -(A - ikB)^{-1}(A + ikB). \tag{4}$$

Let $S = S_v(1)$. Then we have

$$S_v(k) = \frac{(k+1)S + (k-1)I}{(k-1)S + (k+1)I}. \tag{5}$$

This formula was first proven in [23] in a more general case.

We call vertex conditions ***properly connecting*** if the vertex cannot be divided into two (or more) vertices that preserve vertex conditions. For this type of vertex conditions, we have the following theorem.

Theorem 1.5 ([10]): The set of all Hermitian properly connecting vertex condition at the vertex V of degree d can be uniquely parameterized by $d \times d$ irreducible unitary matrices S writing the conditions in the form

$$i(S - I)\vec{\psi} = (S + I)\partial\vec{\psi}. \tag{6}$$

Proof.
From (4) we can take $A = i(S - I)$ and $B = S + I$ such that (A, B) satisfy Theorem . Indeed, AB^* is Hermitian. ∎

We can simplify even further by considering a more special case of vertex conditions, namely, *scaling-invariant* vertex conditions. We call vertex conditions ***scaling-invariant*** if f and any scaling of f satisfy the conditions simultaneously.

The characteristic property of scaling-invariant vertex conditions is that the corresponding vertex scattering matrix is independent of the energy k, i.e. $S_v(k) \equiv S$. Thus, we can work with simpler vertex conditions that do not depend on k. These conditions are described by the following theorem.

Theorem 1.6 ([10]): If vertex conditions are invariant under scaling, S has only two eigenvalues: 1 and -1 and (6) can be written in the form:

$$\begin{cases} P_{-1}\vec{\psi} = 0, \\ P_1\partial\vec{\psi} = 0 \end{cases} \tag{7}$$

where $P_{\pm 1}$ are the eigenprojectors on the two orthogonal eigenspaces of eigenvalues 1 and -1 respectively. In addition, we have

$$S_v(k) = P_1 - P_{-1} = S.$$

Examples of Scattering Matrices

Let us consider our first example: the metric graph $[0, L]$ with the Laplacian. We have one function defined on $E_1 = [0, L]$, which is $\psi(x) = c_1 \cos kx + c_2 \sin kx$. Therefore,

$$\psi(x) = \frac{c_1 i + c_2}{2i} e^{ikx} + \frac{c_1 i - c_2}{2i} e^{-ikx}.$$

Take V^1. The scattering matrix of V^1 is simply a number, since we have only one c_1 and one c_2. Recalling that $c_2 = 0$, so

$$\psi(x) = \frac{c_1}{2} e^{ikx} + \frac{c_1}{2} e^{-ikx}.$$

Thus, if $\frac{c_1}{2} = S\left(\frac{c_1}{2}\right)$ we have $S = 1$. In fact, it is always true if v is of degree 1 with $\psi'(0) = 0$. Indeed, take

$$\psi(x) = c_1 e^{ikx} + c_2 e^{-ikx}, \quad \psi'(0) = 0.$$

Then we can obtain

$$-c_1 ik + c_2 ik = 0 \Rightarrow c_1 = c_2 \Rightarrow S = \frac{c_1}{c_2} = 1.$$

In the case of the Dirichlet condition we have $\psi(0) = c_1 + c_2 = 0$, hence $S = -1$.

Note that in these examples S is independent of k.

1.2. Berry's Phase

We define Berry's phase in the simple case of one cyclic parameter. Let $H(\theta)$ be a smooth family of Hamiltonians depending on a real parameter $\theta \in [0, 2\pi]$, where the parameter space forms a closed loop such that $H(0) = H(2\pi)$. We consider the eigenfunctions of this operator given by the equation:

$$H_\theta \psi = \lambda \psi. \tag{8}$$

As θ changes, both the eigenfunctions and eigenvalues can vary as well. We denote by $\psi^{(\theta)}$ a normalized solution to (8).

The key element is the change any function undergoes as θ traverses the loop. Assume that the eigenfunctions can be chosen real-valued and continuously depending on the parameter θ. Then fixing $\psi^{(\theta)}|_{\theta=0}$ determines the unique eigenfunction $\psi^{(\theta)}$ for any θ. We define the geometric phase ζ by comparing the eigenfunction at the end of the cycle to the beginning:

$$\psi^{(2\pi)} = \lim_{\theta \to 2\pi} \psi^{(\theta)} = e^{i\zeta_\theta} \psi^{(0)}.$$

We call the phase ζ_θ ***geometric*** if it depends only on the path in the domain of H_θ.

The first appearance of Berry's phase happened in the paper by Berry [3]. In that paper, Berry showed the existence of the geometric phase in *adiabatic approximation* — the theorem first mentioned by Ehrenfest in [14] with the first rigorous proof given by Max Born and Vladimir Fock in [12]. Historical context about *adiabatic approximation* can be found in [6].

Application to Metric Graphs

In **Chapter 3**, we will consider a metric graph with a periodic operator matching this setup. If $\psi^{(\theta)}$ is real-valued for all θ, the only possible values for the phase factor $e^{i\zeta_\theta}$ are $+1$ or -1. Consequently, the geometric phase ζ may have just two values:

$$\zeta \equiv 0, \pi \pmod{2\pi}.$$

This gives us a robust topological property of the graph.

Definition 1.7 (Geometric Phase for Real Eigenfunction): Let $H(\theta)$ be a smooth family of self-adjoint operators with $\theta \in [0, 2\pi]$ and $H(0) = H(2\pi)$. For a nondegenerate, normalized, and real-valued eigenfunction $\psi(\theta)$, the ***geometric phase*** ζ is defined by the relation:

$$\psi(2\pi) = e^{i\zeta}\psi(0).$$

In general, the geometric (Berry) phase takes values in $U(1)$ and is defined via parallel transport of eigenstates. In the present setting, due to the existence of a real-valued eigenfunction, this phase reduces to a sign ± 1. A deeper physical introduction on geometric phases can be found in Bohm et al. [4] and Sprinkart et al. [19].

2. Figure-eight Graph

In this chapter, we introduce the metric figure-eight graph and derive its secular equation — the characteristic equation whose roots determine the spectrum of the graph. We further determine eigenfunctions for $k = 0$. These results support work by Tibbling [21].

2.1. Getting Started

We consider the metric figure-eight graph Γ. For convenience, we represent Γ by two segments $[-\ell_1/2, \ell_1/2]$ and $[-\ell_2/2, \ell_2/2]$ forming two edges E_l, E_r joined at the vertex $\mathrm{V} = \{x_1, x_2, x_3, x_4\}$ as follows

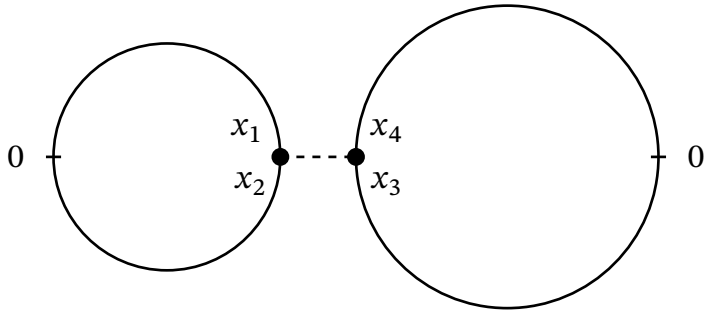

Figure 7: Edges parametrized.

Here, x_1 and x_2 are endpoints of the edge $E_l = [-\ell_1/2, \ell_1/2]$ and x_3, x_4 are the endpoints of the edge $E_r = [-\ell_2/2, \ell_2/2]$. The lengths of the edges are not necessarily equal, although we will focus primarily on studying the case when they are equal. We will denote the graph by Γ^{ℓ_1,ℓ_2} to emphasize the dependence on the lengths of the edges and $\mathcal{L} = \ell_1 + \ell_2$ will be the total length of the graph. If $\ell_1 = \ell_2 = \ell$, we will write Γ^{ℓ}. Sometimes we will omit the lengths in the notation, if it does not cause confusion, and simply write Γ.

We study the Laplacian operator on Γ:

$$L = -\frac{d^2}{dx^2}. \tag{9}$$

To make the operator L self-adjoint, we impose the following vertex conditions:

$$i(S - I)\vec{\psi} = (S + I)\partial\vec{\psi}, \tag{10}$$

where S is any unitary matrix; $\vec{\psi}$ is the vector of limit values and $\partial\vec{\psi}$ is the vector of normal derivatives.

For the figure-eight graph $\vec{\psi}$ and $\partial\vec{\psi}$ are as follows:

$$\vec{\psi} = \begin{pmatrix} \psi_1(x_1) \\ \psi_2(x_2) \\ \psi_3(x_3) \\ \psi_4(x_4) \end{pmatrix} = \begin{pmatrix} \psi_1\left(-\frac{\ell_1}{2}\right) \\ \psi_2\left(\frac{\ell_1}{2}\right) \\ \psi_3\left(-\frac{\ell_2}{2}\right) \\ \psi_4\left(\frac{\ell_2}{2}\right) \end{pmatrix}, \quad \partial\vec{\psi} = \begin{pmatrix} \partial\psi_1(x_1) \\ \partial\psi_2(x_2) \\ \partial\psi_3(x_3) \\ \partial\psi_4(x_4) \end{pmatrix} = \begin{pmatrix} \psi_1'\left(-\frac{\ell_1}{2}\right) \\ -\psi_2'\left(\frac{\ell_1}{2}\right) \\ \psi_3'\left(-\frac{\ell_2}{2}\right) \\ -\psi_4'\left(\frac{\ell_2}{2}\right) \end{pmatrix} \tag{11}$$

where the sign conventions for $\partial\vec{\psi}$ in (11) are illustrated in the following figure:

Figure 8: Sign choice for normal derivatives.

For the problem under consideration, we consider a unitary matrix S that satisfies the Hermitian vertex conditions from Theorem 1.5 and scaling-invariant conditions from Theorem 1.6. This matrix connects points x_1 and x_2 with amplitude β, and x_3 and x_4 with amplitude $-\beta$ and a minus sign due to orientation. We allow direct travel between the loops by connecting x_1 to x_4 and x_2 to x_3, both with amplitude α. However, we prohibit reflections, i.e., $S_{ii} = 0$; and cross-travel, i.e., $S_{13} = S_{31} = S_{24} = S_{42} = 0$.

In this case S is Hermitian and unitary, and thus the spectrum of S is ± 1. Every such unitary matrix can be written as follows [21]:

$$S = \begin{pmatrix} 0 & \beta & 0 & \alpha \\ \beta & 0 & \alpha & 0 \\ 0 & \alpha & 0 & -\beta \\ \alpha & 0 & -\beta & 0 \end{pmatrix}, \quad \alpha^2 + \beta^2 = 1. \tag{12}$$

It is easier to parametrize α and β using a single parameter $\theta \in [0, 2\pi]$ so that $(\alpha, \beta) = (\cos\theta, \sin\theta)$; for any fixed θ, the scattering matrix is defined by S_θ as follows:

$$S_\theta = \begin{pmatrix} 0 & \sin\theta & 0 & \cos\theta \\ \sin\theta & 0 & \cos\theta & 0 \\ 0 & \cos\theta & 0 & -\sin\theta \\ \cos\theta & 0 & -\sin\theta & 0 \end{pmatrix}$$

From now on, we will be working with θ-dependent vertex conditions:

$$i(S_\theta - I)\vec{\psi} = (S_\theta + I)\partial\vec{\psi}. \tag{13}$$

The constructed system is 2π-periodic with respect to θ. Therefore, we might investigate *the existence of Berry's phase*. Also note that these vertex conditions connect the vertex values at all four endpoints and, thus, are properly connecting, except in four cases when topology changes; namely, when $\theta = 0, \pi/2, 3\pi/2$, or 2π. These four cases give special vertex conditions connecting vertices with coefficients ± 1 (we depict -1 by a black dot on the Figure 9). This leads to a model of topology change that is similar to Cheon et al. [5]:

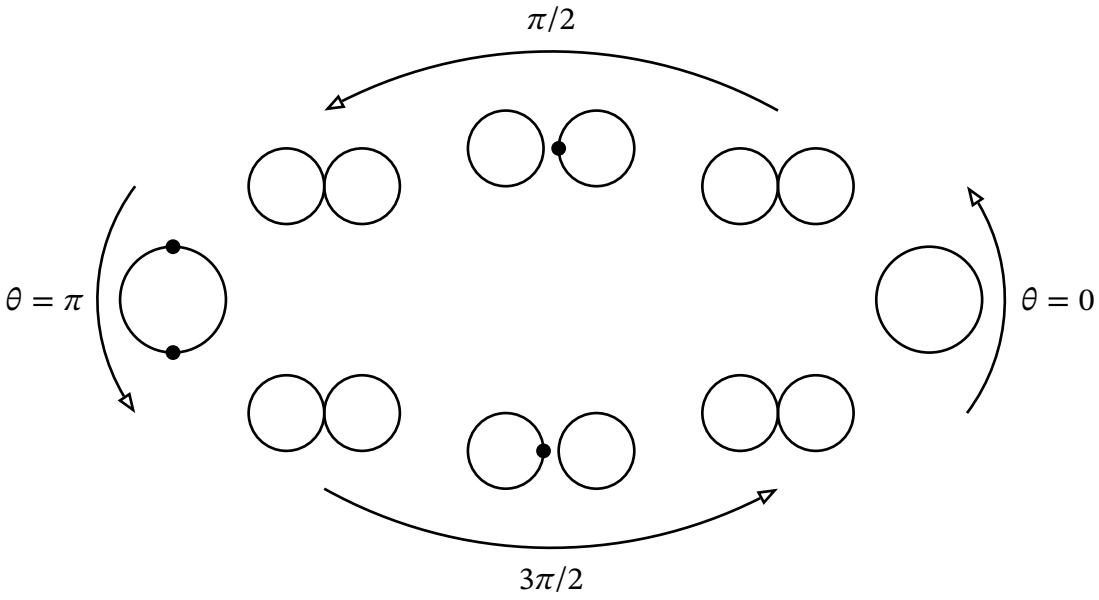

Figure 9: Cycle of topological changes corresponding to S_θ.

The differential operator L from (9) with the domain defined by the new vertex conditions (13) will be denoted by L_θ. Then the eigenvalues of operator L_θ can be calculated by solving the following equation:

$$L_\theta\psi(x) = \lambda(\theta)\psi(x), \tag{14}$$

on each of E_l and E_r.

We denote a metric graph formed by the operator L_θ and vertex conditions (13) as $\Gamma_\theta^{\ell_1,\ell_2}$.

2.2. Graph Symmetry

The figure-eight graph has two reflection symmetries similar to a rectangle. However, our vertex conditions are not completely symmetric along the vertical line through point V, since matrix S_θ connects edges differently depending on the parameter θ. Geometrically, the symmetry is preserved; however, the vertex conditions can be asymmetric.

We turn to the horizontal symmetry $Jf(x) \coloneqq f(-x)$. This symmetry satisfies $J^2 = I$ by definition.

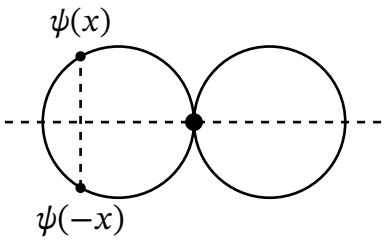

Figure 10: J-symmetry.

Let us take the limit values $\vec{\psi}$ of a function ψ, then $J\vec{\psi}$ is given by the unitary matrix

$$J = \begin{pmatrix} 0 & 1 & 0 & 0 \\ 1 & 0 & 0 & 0 \\ 0 & 0 & 0 & 1 \\ 0 & 0 & 1 & 0 \end{pmatrix}.$$

Thus, we can act by J on the vertex conditions (13) and, since $JSJ = S$, this symmetry does not change the space of eigenfunctions. Therefore, one can choose eigenfunctions to be either even or odd with respect to the symmetry J.

- Even: $\psi_{\text{even}}(x) = \frac{1}{2}(\psi(x) + \psi(-x))$
- Odd: $\psi_{\text{odd}}(x) = \frac{1}{2}(\psi(x) - \psi(-x))$

By definition of our model, the eigenfunctions of the graph Γ_θ are solutions to the differential equation

$$-\psi'' = \lambda\psi, \quad \lambda = k^2 \tag{15}$$

satisfying the vertex conditions (13). The general solutions of (15) are $c_1 \cos kx + c_2 \sin kx$. Hence, the eigenfunctions that satisfy (14) can be chosen as follows:

$$\psi_{\text{even}}(x) = a \cos kx, \quad \psi_{\text{odd}}(x) = b \sin kx.$$

This leads to a significant simplification of the problem. Indeed, using notation from (11) we have $\psi_s^e(x) = a_s \cos kx$ or $\psi_s^o(x) = b_s \sin kx$, where $s \in \{l, r\}$ and $\lambda = k^2$.

2.3. Secular Equation

The next step is to derive the secular equation — the equation describing the spectrum of Γ_θ. We start with the general case when $\alpha \neq 0$ and then consider the special case.

General Case $\alpha \neq 0$

Even Eigenfunctions

We start with the even basis (ψ is a cosine). One can see that for an even function $\psi(x_1) = \psi(x_2)$ and $\psi(x_3) = \psi(x_4)$ which yields

$$\vec{\psi} = \begin{pmatrix} a_l \cos \ell_1 k/2 \\ a_l \cos \ell_1 k/2 \\ a_r \cos \ell_2 k/2 \\ a_r \cos \ell_2 k/2 \end{pmatrix} \quad \partial\vec{\psi} = k \begin{pmatrix} a_l \sin \ell_1 k/2 \\ a_l \sin \ell_1 k/2 \\ a_r \sin \ell_2 k/2 \\ a_r \sin \ell_2 k/2 \end{pmatrix} \tag{16}$$

In Kurasov [10] it was proven that if the scattering matrix S does not depend on the energy, then

$$S = P_1 - P_{-1}.$$

Consequently, the vertex conditions (13) are equivalent to

$$P_1 \partial\vec{\psi} = P_{-1}\vec{\psi} = 0. \tag{17}$$

One can check that $P_1 = 1/2(S + I)$ and $P_{-1} = 1/2(S - I)$.

The equation for the eigenvalues of the matrix S is

$$\det(S_\theta - \lambda I) = \left(\alpha^2 + \beta^2 - \lambda^2\right)^2 = (\lambda - 1)^2(\lambda + 1)^2.$$

Since the multiplicity of both eigenvalues is two, it follows that the ranks of the corresponding operators $P_1\partial\vec{\psi}$ and $P_{-1}\vec{\psi}$ are also two. Hence, we can consider a simplified system of equations by taking only the first two rows in (17):

$$\begin{pmatrix} -1 & \beta & 0 & \alpha \\ \beta & -1 & \alpha & 0 \end{pmatrix} \begin{pmatrix} a_l \cos(\ell_1 k/2) \\ a_l \cos(\ell_1 k/2) \\ a_r \cos(\ell_2 k/2) \\ a_r \cos(\ell_2 k/2) \end{pmatrix} = 0, \quad \begin{pmatrix} 1 & \beta & 0 & \alpha \\ \beta & 1 & \alpha & 0 \end{pmatrix} \begin{pmatrix} a_l \sin(\ell_1 k/2) \\ a_l \sin(\ell_1 k/2) \\ a_r \sin(\ell_2 k/2) \\ a_r \sin(\ell_2 k/2) \end{pmatrix} = 0.$$

This, in turn, yields the following equations

$$\begin{pmatrix} (-1 + \beta)\cos(\ell_1 k/2) & \alpha \cos(\ell_2 k/2) \\ (1 + \beta)\sin(\ell_1 k/2) & \alpha \sin(\ell_2 k/2) \end{pmatrix} \begin{pmatrix} a_l \\ a_r \end{pmatrix} = 0 \tag{18}$$

One can see, these equations hold only when α is non-zero. Otherwise, they become degenerate as the first two rows become linearly dependent.

A non-trivial solution exists when the determinant of the matrix is zero:

$$\begin{aligned}&\det\begin{pmatrix}(-1+\beta)\cos(\ell_1 k/2) & \alpha\cos(\ell_2 k/2)\\ (1+\beta)\sin(\ell_1 k/2) & \alpha\sin(\ell_2 k/2)\end{pmatrix} = \alpha\cdot\\ &\left[(-1+\beta)\cos\left(\frac{\ell_1 k}{2}\right)\sin\left(\frac{\ell_2 k}{2}\right) - (1+\beta)\cos\left(\frac{\ell_2 k}{2}\right)\sin\left(\frac{\ell_1 k}{2}\right)\right]\\ &= \alpha\beta\sin((\ell_2-\ell_1)k/2) - \alpha\sin((\ell_2+\ell_1)k/2).\end{aligned} \tag{19}$$

If $\ell_1 = \ell_2 = \ell$, then the secular equation becomes

$$\alpha\sin(\ell k) = 0 \tag{20}$$

which gives simple eigenvalues $k_n = \pi n/\ell$, where $\lambda_n = k_n^2$.

Odd Eigenfunctions

For the odd basis (ψ is a sine), we similarly obtain

$$\vec{\psi} = \begin{pmatrix}-a_l\sin\ell_1 k/2\\ a_l\sin\ell_1 k/2\\ -a_r\sin\ell_2 k/2\\ a_r\sin\ell_2 k/2\end{pmatrix} \quad \partial\vec{\psi} = k\begin{pmatrix}a_l\cos\ell_1 k/2\\ -a_l\cos\ell_1 k/2\\ a_r\cos\ell_2 k/2\\ -a_r\cos\ell_2 k/2\end{pmatrix} \tag{21}$$

Exactly as before, this yields the following equations for coefficients a_l and a_r:

$$\begin{pmatrix}(1+\beta)\sin(\ell_1 k/2) & \alpha\sin(\ell_2 k/2)\\ (1-\beta)\cos(\ell_1 k/2) & -\alpha\cos(\ell_2 k/2)\end{pmatrix}\begin{pmatrix}a_l\\ a_r\end{pmatrix} = 0$$

This leads to the same secular equation as before:

$$\begin{aligned}&\det\begin{pmatrix}(1+\beta)\sin(\ell_1 k/2) & \alpha\sin(\ell_2 k/2)\\ (1-\beta)\cos(\ell_1 k/2) & -\alpha\cos(\ell_2 k/2)\end{pmatrix} =\\ &= \alpha\beta\sin((\ell_2-\ell_1)k/2) - \alpha\sin((\ell_2+\ell_1)k/2).\end{aligned} \tag{22}$$

As demonstrated above, this secular equation does not describe the case when $\alpha = 0$, since the system becomes degenerate. We need to use a different equation.

Special Case $\alpha = 0$

Even Eigenfunctions

For the case $\theta = \pi/2$, we can take the second and third rows, which yield the following equation for even functions

$$\begin{pmatrix} \beta & -1 & \alpha & 0 \\ 0 & \alpha & -1 & -\beta \end{pmatrix} \begin{pmatrix} a_l \cos(\ell_1 k/2) \\ a_l \cos(\ell_1 k/2) \\ a_r \cos(\ell_2 k/2) \\ a_r \cos(\ell_2 k/2) \end{pmatrix} = 0, \quad \begin{pmatrix} \beta & 1 & \alpha & 0 \\ 0 & \alpha & 1 & -\beta \end{pmatrix} \begin{pmatrix} a_l \sin(\ell_1 k/2) \\ a_l \sin(\ell_1 k/2) \\ a_r \sin(\ell_2 k/2) \\ a_r \sin(\ell_2 k/2) \end{pmatrix} = 0.$$

As $\alpha = 0$ we get

$$\det \begin{pmatrix} (\beta - 1)\cos(\ell_1 k/2) & -(1+\beta)\cos(\ell_2 k/2) \\ (\beta + 1)\sin(\ell_1 k/2) & (1-\beta)\sin(\ell_2 k/2) \end{pmatrix} = 0$$

and since $\beta = 1$ when $\theta = \pi/2$, the final equation is

$$\sin(\ell_1 k/2)\cos(\ell_2 k/2) = 0.$$

Therefore, $\Gamma_{\pi/2}$ has two sets of eigenvalues:

$$\{2n\pi/\ell_1 : n = 1, 2, ...\} \text{ and } \{(2n+1)\pi/\ell_2 : n = 1, 2, ...\}.$$

One can easily see that for $\Gamma_{3\pi/2}$, when $\beta = -1$, the secular equation exchanges the roles of ℓ_1 and ℓ_2 as follows:

$$\sin(\ell_2 k/2)\cos(\ell_1 k/2) = 0$$

and we get: $\{(2n+1)\pi/\ell_1 : n = 1, 2, ...\}$ and $\{2n\pi/\ell_2 : n = 1, 2, ...\}$.

Odd Eigenfunctions

The equation for odd functions takes the following form:

$$\begin{pmatrix} \beta & -1 & \alpha & 0 \\ 0 & \alpha & -1 & -\beta \end{pmatrix} \begin{pmatrix} -a_l \sin \ell_1 k/2 \\ a_l \sin \ell_1 k/2 \\ -a_r \sin \ell_2 k/2 \\ a_r \sin \ell_2 k/2 \end{pmatrix} = 0, \quad \begin{pmatrix} \beta & 1 & \alpha & 0 \\ 0 & \alpha & 1 & -\beta \end{pmatrix} \begin{pmatrix} a_l \cos \ell_1 k/2 \\ -a_l \cos \ell_1 k/2 \\ a_r \cos \ell_2 k/2 \\ -a_r \cos \ell_2 k/2 \end{pmatrix} = 0.$$

We get the following secular equation:

$$\det \begin{pmatrix} -(\beta+1)\sin(\ell_1 k/2) & (1-\beta)\sin(\ell_2 k/2) \\ (\beta-1)\cos(\ell_1 k/2) & (1+\beta)\cos(\ell_2 k/2) \end{pmatrix} = 0.$$

Therefore,

$$\begin{aligned}\theta = \pi/2: &\quad \sin(\ell_1 k/2)\cos(\ell_2 k/2) = 0,\\ \theta = 3\pi/2: &\quad \sin(\ell_2 k/2)\cos(\ell_1 k/2) = 0.\end{aligned}$$

and eigenvalues are similar to the previous case.

Eigenfunctions for $\lambda = 0$

Let us turn to the calculation of the spectral multiplicity of $k = 0$, i.e., the number of linearly independent eigenfunctions corresponding to equation (9).

All solutions to the differential equation are then given by:

$$\psi(x) = \begin{cases} a_l x + b_l, & x \in E_l; \\ a_r x + b_r, & x \in E_r. \end{cases}$$

Consequently, even and odd eigenfunctions are

$$\psi^e(x) = \frac{1}{2}(\psi(x) + \psi(-x)) = \begin{cases} b_l, & x \in E_l; \\ b_r, & x \in E_r \end{cases}$$

$$\psi^o(x) = \frac{1}{2}(\psi(x) - \psi(-x)) = \begin{cases} a_l x, & x \in E_l; \\ a_r x, & x \in E_r \end{cases}$$

Even Eigenfunctions

The limit values are as follows:

$$\vec{\psi}^e = \begin{pmatrix} b_l \\ b_l \\ b_r \\ b_r \end{pmatrix}, \quad \partial\vec{\psi}^e = \begin{pmatrix} 0 \\ 0 \\ 0 \\ 0 \end{pmatrix}.$$

For the even basis, we obtain the system

$$\begin{aligned}(-1 + \beta)b_l + \alpha b_r = 0,\\ 0 = 0.\end{aligned} \tag{23}$$

The normalization is

$$1 = \|\psi\|_2^2 = b_l^2 \int_{-\frac{\ell_1}{2}}^{\frac{\ell_1}{2}} \mathrm{d}x + b_r^2 \int_{-\frac{\ell_2}{2}}^{\frac{\ell_2}{2}} \mathrm{d}x = \ell_1 b_l^2 + \ell_2 b_r^2.$$

Therefore, we have the following system of equations:

$$(1+\beta)(1-\beta)b_l + \alpha(1+\beta)b_r = \alpha b_l - (1+\beta)b_r = 0,$$
$$b_l^2\ell_1 + \ell_2 b_r^2 = 1.$$

This leads to the solution

$$b_l = \sqrt{\frac{(1+\beta)^2}{\alpha^2\ell_1 + (1+\beta)^2\ell_2}}, \quad b_r = \sqrt{\frac{\alpha^2}{\alpha^2\ell_1 + (1+\beta)^2\ell_2}}. \tag{24}$$

We get an indeterminate form $\frac{0}{0}$ when $\theta \to 3\pi/2$, i.e., $\alpha \to 0$ and $\beta \to -1$. Computing this limit directly, we get:

$$\lim_{\theta\to\frac{3\pi}{2}} b_l(\theta) = \lim_{\theta\to\frac{3\pi}{2}} b_r(\theta) = \frac{1}{\sqrt{\ell_1+\ell_2}}.$$

Odd Eigenfunctions

For the odd eigenfunction, the limit values are

$$\vec{\psi}^o = \begin{pmatrix} -a_l\frac{\ell_1}{2} \\ a_l\frac{\ell_1}{2} \\ -a_r\frac{\ell_2}{2} \\ a_r\frac{\ell_2}{2} \end{pmatrix}, \quad \partial\vec{\psi}^o = \begin{pmatrix} a_l \\ -a_l \\ a_r \\ -a_r \end{pmatrix}.$$

For odd eigenfunctions we get the following system of equations:

$$(1+\beta)\frac{a_l\ell_1}{2} + \alpha\frac{a_r\ell_2}{2} = 0,$$
$$(-1+\beta)a_l + \alpha a_r = 0,$$

which leads to $a_l = a_r = 0$; thus, there are no odd eigenfunctions corresponding to $\lambda = 0$.

By combining all the results of this section, we obtain the following theorem.

Theorem 2.1: The figure-eight graph $\Gamma_\theta^{\ell_1,\ell_2}$ with θ-dependent vertex conditions (13) has the following secular equations describing its spectrum:

$$\theta \neq \pi/2, 3\pi/2 : \beta \sin\left(\frac{(\ell_2-\ell_1)k}{2}\right) - \sin\left(\frac{(\ell_2+\ell_1)k}{2}\right) = 0,$$
$$\theta = \pi/2 : \qquad \sin(\ell_1 k/2)\cos(\ell_2 k/2) = 0,$$
$$\theta = 3\pi/2 : \qquad \sin(\ell_2 k/2)\cos(\ell_1 k/2) = 0.$$

All k except 0 have multiplicity two. For 0 the multiplicity is one.

We note that the spectrum for $\theta = \pi/2$ is as follows

$$\left\{\frac{2n\pi}{\ell_1} : n = 0, 1, \ldots\right\} \cup \left\{\frac{(2n+1)\pi}{\ell_2} : n = 0, 1, \ldots\right\}.$$

and, in the case $\theta = \pi$, the spectrum is

$$\left\{\frac{2n\pi}{\ell_1+\ell_2} : n = 0, 1, \ldots\right\}.$$

It is convenient to consider the case $\ell_1 = \ell_2$ to obtain a consistent spectrum. In that case we can study Berry's phase for a fixed eigenvalue k. That is not strictly necessary, but we study this case for convenience.

3. Berry's Phase

In this chapter, we use the model of topology change constructed in **Chapter 2** to explicitly compute the eigenfunction coefficients as functions of θ and prove the existence of Berry's phase π. This result confirms Tibbling's hypothesis [21].

As introduced in **Section 1.2**, Berry's phase requires a continuous change defined by $e^{i\zeta_\theta}$, where ζ_θ is a parameter depending on θ. However, we work with $L_\theta = -\frac{d^2}{dx^2}$, thus, the eigenfunctions are real and ζ_θ can be 0 or $\pi \pmod{2\pi}$.

3.1. Phase for Equal Lengths

Now we consider the case where $\ell_1 = \ell_2 = \ell$. In this case, for any θ the secular equation (20) yields double eigenvalues, namely, $k_n = \pi n/\ell$ for $n = 1, 2, \ldots$. The only quantities left to determine are the coefficients a_l and a_r in the case of the even eigenfunctions and b_l and b_r in the case of odd eigenfunctions. Since their equations depend on $\cos k\ell$ and $\sin k\ell$, we have to consider two cases: when n is even and when n is odd. Due to the periodicity of the sine and cosine functions, it suffices to consider $k = \pi/\ell$ and $k = 2\pi/\ell$. One can then verify that

$$\begin{aligned} \text{even}: &\quad \begin{cases} k = \pi/\ell: & (1+\beta)a_l + \alpha a_r = 0, \\ k = 2\pi/\ell: & (-1+\beta)a_l + \alpha a_r = 0. \end{cases} \\ \text{odd}: &\quad \begin{cases} k = \pi/\ell: & (1+\beta)b_l + \alpha b_r = 0, \\ k = 2\pi/\ell: & (-1+\beta)b_l + \alpha b_r = 0. \end{cases} \end{aligned} \tag{25}$$

Even Eigenfunctions

Let $k = \pi/\ell$. Then, for the even eigenfunctions we have

$$(1+\beta)a_l + \alpha a_r = 0.$$

This equation has a unique solution up to a phase factor $e^{i\zeta_\theta}$ provided that ψ is normalized:

$$\|\psi\|_2^2 = (a_l^2 + a_r^2)\int_{-\frac{\ell}{2}}^{\frac{\ell}{2}} \cos^2(\pi n x/\ell)\,\mathrm{d}x = \frac{1}{2}(a_l^2 + a_r^2).$$

Therefore, our system of equations is

$$\begin{aligned}(1+\beta)a_l + \alpha a_r &= 0,\\ a_l^2 + a_r^2 &= 2.\end{aligned} \tag{26}$$

The eigenfunction depends on the parameter θ, and we need to choose a continuous parametrization. The eigenfunction for $\theta = 0$ can be chosen arbitrarily; we then obtain a continuous family of eigenfunctions with a unique eigenfunction for each θ. Thus, we seek $a_{l,r} \in \mathbb{R}$ and $b_{l,r} \in \mathbb{R}$ that depend continuously on θ.

Equations (26) can be solved geometrically as follows. Consider a table for all θ:

θ	0	$\left(0, \frac{\pi}{2}\right)$	$\frac{\pi}{2}$	$\left(\frac{\pi}{2}, \pi\right)$	π	$\left(\pi, \frac{3\pi}{2}\right)$	$\frac{3\pi}{2}$	$\left(\frac{3\pi}{2}, 2\pi\right)$
α	1	$+$	0	$-$	-1	$-$	0	$+$
β	0	$+$	1	$+$	0	$-$	-1	$-$
a_l	1	$+$	0	$-$	-1	$-$	$-\sqrt{2}$	$\to -1$
a_r	-1	$-$	$-\sqrt{2}$	$-$	-1	$-$	0	$\to 1$

Table 1: Behavior of a_l and a_r for $k = \pi/\ell$.

where $+$ indicates that the parameter is positive on the interval and $-$ indicates that it is negative.

This table shows solutions of (26) for special points and the signs for all parameters in the intervals. This suffices to demonstrate that a continuous solution exists.

For the case $\theta = 3\pi/2$, determining a_l and a_r from the equation is problematic. To resolve this, we rewrite the equation as follows:

$$\begin{aligned}&(1-\beta)(1+\beta)a_l + \alpha(1-\beta)a_r = 0\\ \Rightarrow\ &\alpha a_l + (1-\beta)a_r = 0.\end{aligned}$$

This yields $a_l = \sqrt{2}$ and $a_r = 0$ for $\theta = 3\pi/2$. Now we can find a_l and a_r as continuous functions depending on θ. Indeed, we get

$$a_l^2 = -\frac{(1-\beta)^2}{\alpha^2} a_r^2 = -\frac{1-\beta}{1+\beta} a_r^2.$$

This equation can be substituted into normalization equation in (26). Note that squares give an ambiguity of the sign, which is why we constructed an explicit continuous solution.

Thus, for $k = \pi/\ell$, we obtain the solution

$$a_l = \varepsilon(\theta)\frac{\cos\theta}{\sqrt{1+\sin\theta}}, \quad a_r = \varepsilon(\theta)\sqrt{1+\sin(\theta)},$$

where $\varepsilon(\theta)$ is a sign function defined as follows

$$\varepsilon(\theta) = \begin{cases} 1, & 0 \le \theta < \frac{3\pi}{2}, \\ -1, & \frac{3\pi}{2} \le \theta < 2\pi. \end{cases} \tag{27}$$

We determine $\varepsilon(\theta)$ according to Table 1. This function appears since from the system (26) we cannot determine the sign for the continuous solution. As we shall see $\varepsilon(\theta)$ yields a continuous solution.

Analogously, the system for $k = 2\pi/\ell$ is

$$\begin{aligned} (-1+\beta)a_l + \alpha a_r &= 0, \\ a_l^2 + a_r^2 &= 2. \end{aligned} \tag{28}$$

This yields a table similar to the previous:

θ	0	$\left(0, \frac{\pi}{2}\right)$	$\frac{\pi}{2}$	$\left(\frac{\pi}{2}, \pi\right)$	π	$\left(\pi, \frac{3\pi}{2}\right)$	$\frac{3\pi}{2}$	$\left(\frac{3\pi}{2}, 2\pi\right)$
α	1	+	0	−	−1	−	0	+
β	0	+	1	+	0	−	−1	−
a_r	1	+	$\sqrt{2}$	+	1	+	0	$\to -1$
a_l	1	+	0	−	−1	−	$-\sqrt{2}$	$\to -1$

Table 2: Behavior of a_l and a_r for $k = 2\pi/\ell$.

For $\theta = \pi/2$ finding a_l and a_r is not possible for the same reason as before. Thus, we rewrite the equation as follows:

$$(1+\beta)(-1+\beta)a_l + (1+\beta)\alpha a_r = -\alpha a_l + (1+\beta)a_r = 0.$$

This equation yields $a_l = 0$ and $a_r = \sqrt{2}$ for $\theta = \pi/2$.

This shows that a continuous solution exists. Now we turn to precise calculation. For both cases, this is relatively straightforward. Indeed, from (26):

$$\begin{aligned}(1+\beta)^2 a_l^2 &= \alpha^2 a_r^2 \\ \Rightarrow 2(1+\beta)^2 &= (1+\beta)^2 a_r^2 + \alpha^2 a_r^2 \\ \Rightarrow (1+\beta)^2 &= (1+\beta) a_r^2.\end{aligned}$$

For $k = 2\pi/\ell$, similar calculations yield the following solution:

$$a_l = \varepsilon(\theta)\frac{\cos\theta}{\sqrt{1+\sin\theta}}, \quad a_r = -\varepsilon(\theta)\sqrt{1+\sin(\theta)},$$

where $\varepsilon(\theta)$ is defined in (27). The continuous solutions for each case are shown in the following figures.

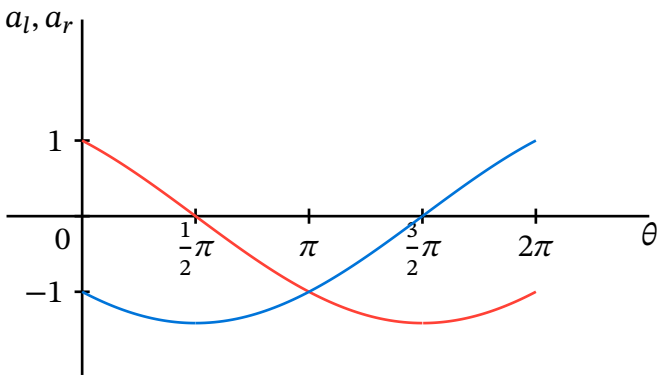

Figure 11: Graph of a_l (red) and a_r (blue) for $k = \pi/\ell$.

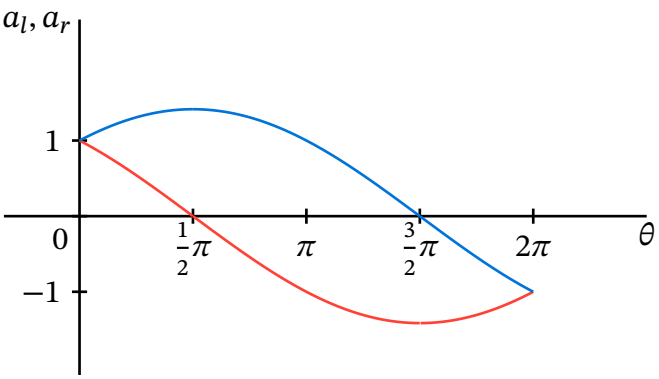

Figure 12: Graph of a_l (red) and a_r (blue) for $k = 2\pi/\ell$.

The continuous solutions for both cases show that after one cycle $\theta : 0 \to 2\pi$ the eigenfunction changes its sign; thus, Berry's phase is π for all even eigenfunctions with $k \neq 0$:

$$\psi_k^{(2\pi)}(x) = e^{i\pi}\psi_k^{(0)},$$

where $\psi_k(x) = \begin{pmatrix} a_l \cos kx \\ a_r \cos kx \end{pmatrix}$ and a_l, a_r are defined for each k as continuous functions depending on θ:

$$k = (\pi + 2\pi n)/\ell : a_l = \varepsilon(\theta)\frac{\cos(\theta)}{\sqrt{1+\sin\theta}}, \quad a_r = \varepsilon(\theta)\sqrt{1+\sin\theta};$$

$$k = 2n\pi/\ell : \qquad a_l = \varepsilon(\theta)\frac{\cos\theta}{\sqrt{1+\sin\theta}}, \quad a_r = -\varepsilon(\theta)\sqrt{1+\sin\theta},$$

for $n = 1, 2, \ldots$.

Odd Eigenfunctions

The system of equations in (25) is essentially the same for odd eigenfunctions, and therefore all reasoning is identical to that for even eigenfunctions. Berry's phase is π for all odd eigenfunctions with $k \neq 0$:

$$\psi_k^{(2\pi)}(x) = e^{i\pi}\psi_k^{(0)},$$

where $\psi_k(x) = \begin{pmatrix} b_l \sin kx \\ b_r \sin kx \end{pmatrix}$ and b_l, b_r are defined for each k as follows:

$$k = (\pi + 2\pi n)/\ell : b_l = \varepsilon(\theta)\frac{\cos(\theta)}{\sqrt{1+\sin\theta}}, \quad b_r = \varepsilon(\theta)\sqrt{1+\sin\theta};$$

$$k = 2n\pi/\ell : \qquad b_l = \varepsilon(\theta)\frac{\cos\theta}{\sqrt{1+\sin\theta}}, \quad b_r = -\varepsilon(\theta)\sqrt{1+\sin\theta},$$

for $n = 1, 2, \ldots$.

It remains to determine the existence of Berry's phase for $k = 0$.

Eigenfunctions for $k = 0$

As we determined earlier, our model has no odd eigenfunctions. Thus, we consider only even eigenfunctions. We have the general solution (24); for $\ell_1 = \ell_2$, this solution yields

$$b_l = \frac{\varepsilon(\theta)}{\sqrt{2\ell}}\frac{\cos\theta}{\sqrt{1+\sin\theta}}, \quad b_r = -\frac{\varepsilon(\theta)}{\sqrt{2\ell}}\sqrt{1+\sin(\theta)},$$

where $\varepsilon(\theta)$ is the same sign function defined in (27). Hence, the zeroth eigenfunction exists for all θ and the phase is also π:

$$\psi_0^{(2\pi)} = e^{i\pi}\psi_0^{(0)}.$$

We can now summarize the results of this section in the following theorem.

Theorem 3.1: For the figure-eight graph Γ_θ^ℓ with equal lengths of edges and θ-dependent vertex conditions (13), Berry's phase after one cycle $\theta : 0 \to 2\pi$ is π for both even and odd eigenfunctions.

This result appears to contradict the claim by Shapere et al. in [16], where the authors claimed that no Berry's phase occurs for graph models with real-valued eigenfunctions.

3.2. Phase for Unequal Lengths

It is natural to ask what happens if the lengths of the edges are not equal. It is equally natural to formulate the following conjecture based on our calculations:

Hypothesis 3.2: For $\ell_1 \neq \ell_2$ the figure-eight graph $\Gamma_\theta^{(\ell_1,\ell_2)}$ acquires Berry's phase π after a full cycle $\theta : 0 \to 2\pi$, for all eigenfunctions including $k = 0$.

Although the case where $\ell_1 \neq \ell_2$ does not have a fixed spectrum under θ (for example Figure 14 shows spectrum of $\Gamma_\theta^{(\pi,1/\pi)}$), there are reasons to believe that Berry's phase is π for any appropriate values of ℓ_1 and ℓ_2. This hypothesis comes from the $k = 0$ solution (24) and the and the continuity of the spectrum as a function of θ.

Equation (24) shows Berry's phase for any ℓ_1 and ℓ_2 as illustrated by the following figure.

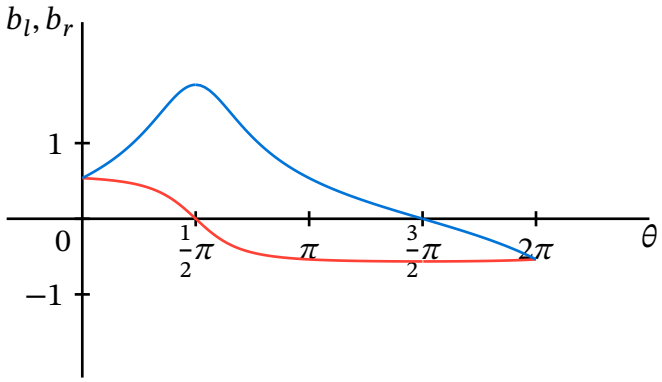

Figure 13: Graph of b_l (red) and b_r (blue) for $k = 0$ and $\ell_1 = \pi$, $\ell_2 = 1/\pi$.

Indeed, even for different lengths, the phase remains. By varying ℓ_1 and ℓ_2 we can change peaks on the graph, but not the phase. This continuity suggests that the same picture holds for other values of k.

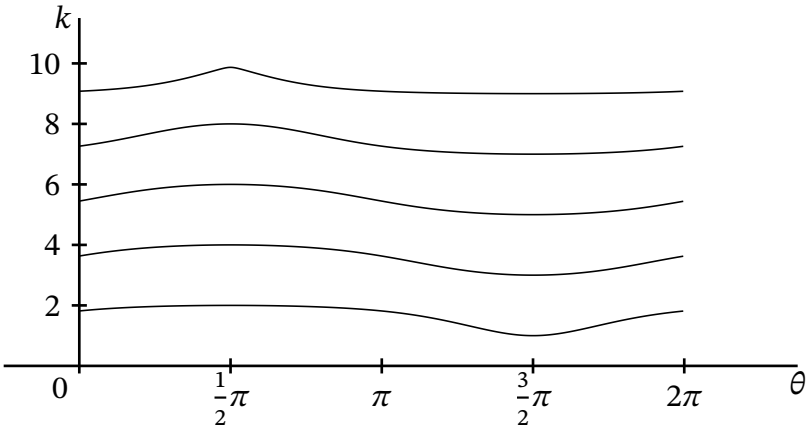

Figure 14: Spectrum of $\Gamma_\theta^{\pi,1/\pi}$ as a function of θ.

It follows that the $k = 0$ solution has Berry's phase π even when $\ell_1 \neq \ell_2$. However, this has not been proven for $k \neq 0$ and remains an open question.

Conclusion

Throughout this thesis, we have introduced a new model of topology change for the metric figure-eight graph. We explored the influence of the topology of quantum graphs on spectral properties, which stem from the works by Balachandran et al. [1] and by Shapere et al. [16]. Shapere et al. also claimed that such a system does not have Berry's phase, even though the eigenfunctions can be chosen to be real-valued. In contrast to this claim, our model of the figure-eight graph has Berry's phase π, which confirms observations made by Tibbling [21].

The simplicity of our model is one of the distinctive features in comparison to previous models, which makes the presence of Berry's phase even more interesting. We rigorously derived the secular equation and the eigenfunctions for the parameter θ. We supplied rigorous derivations for results consistent with the parametrization used by Tibbling [21].

Another direction for future research is the generalization of the figure-eight graph to the flower graph (one vertex and n edges). While flower graphs were explored to some extent in Fujimoto et al. [8] and Inoue et al. [9] for the Dirac operator, the question regarding the structure of topology change and the existence of Berry's phase for those graphs remains largely unresolved.

Another interesting question is whether a magnetic field influences Berry's phase. As we mentioned in **Section 2.1**, Kurasov and Serio in [11] established that the figure-eight graph with a magnetic field and the fluxes φ_1 and φ_2 of the edges E_l and E_r respectively, has a notable feature: whenever one of the fluxes is zero, the magnetic field has no influence on the spectrum. This provides an example of a system similar to ours in which the magnetic field has a notable effect.

Finally, our setting has direct implications for experimental physics. This opens the possibility of an experimental verification that could lend further support to this work.

Bibliography

[1] A. P. Balachandran, G. Bimonte, G. Marmo, and A. Simoni, "Topology change and quantum physics," *Nuclear Physics B*, vol. 446, no. 1–2, pp. 299–314, 1995, doi: 10.1016/0550-3213(95)00260-Y.

[2] G. Berkolaiko, "An elementary introduction to quantum graphs," *arXiv preprint*, 2016, [Online]. Available at: https://arxiv.org/abs/1603.07356

[3] M. V. Berry, "Quantal phase factors accompanying adiabatic changes," *Proceedings of the Royal Society A: Mathematical and Physical Sciences*, vol. 392, pp. 45–57, 1984, doi: 10.1098/rspa.1984.0023.

[4] A. Bohm, A. Mostafazadeh, H. Koizumi, Q. Niu, and J. Zwanziger, *The Geometric Phase in Quantum Systems: Foundations, Mathematical Concepts, and Applications in Molecular and Condensed Matter Physics*, 1st ed. Springer Berlin, Heidelberg, 2003. doi: 10.1007/978-3-662-10333-3.

[5] T. Cheon, A. Tanaka, and O. Turek, "Example of quantum holonomy with topology change," *Acta Polytechnica*, vol. 53, no. 5, pp. 410–415, 2013, doi: 10.14311/AP.2013.53.0410.

[6] K. Durstberger, "Geometric Phases in Quantum Theory," Doctoral dissertation, 2002. [Online]. Available at: https://physics.gu.se/~tfkhj/Durstberger.pdf

[7] Eugene P. Wigner, "The Unreasonable Effectiveness of Mathematics in the Natural Sciences," *Communications on Pure and Applied Mathematics*, vol. 13, pp. 1–14, 1960, doi: 10.1002/cpa.3160130102.

[8] Y. Fujimoto, T. Inoue, M. Sakamoto, K. Takenaga, and I. Ueba, "5d Dirac fermion on quantum graph," *Journal of Physics A: Mathematical and Theoretical*, vol. 52, no. 455401, 2019, doi: 10.1088/1751-8121/ab4859.

[9] T. Inoue, M. Sakamoto, and I. Ueba, "Instantons and Berry's connections on quantum graph," *Journal of Physics A: Mathematical and Theoretical*, vol. 54, no. 355301, 2021, doi: 10.1088/1751-8121/ac17a3.

[10] P. Kurasov, *Spectral Geometry of Graphs*, 1st ed. Springer Berlin Heidelberg, 2024.

[11] P. Kurasov and A. Serio, "Topological damping of Aharonov-Bohm effect: quantum graphs and vertex conditions," *Nanosystems: Physics, Chemistry, Mathematics*, vol. 6, no. 3, pp. 309–319, 2015, doi: 10.17586/2220-8054-2015-6-3-309-319.

[12] M. Born and V. Fock, "Beweis des Adiabatensatzes," *Zeitschrift für Physik*, vol. 51, pp. 165–180, 1928, doi: 10.1007/BF01343193.

[13] D. U. Matrasulov, J. R. Yusupov, K. K. Sabirov, and Z. A. Sobirov, "Time-dependent quantum graph," *Nanosystems: Physics, Chemistry, Mathematics*, vol. 6, no. 2, pp. 173–181, 2015, doi: 10.17586/2220-8054-2015-6-2-173-181.

[14] P. Ehrenfest, "Adiabatische Invarianten und Quantentheorie," *Annalen der Physik*, vol. 356, pp. 327–352, 1916, doi: 10.1002/andp.19163561905.

[15] J. J. Sakurai and J. Napolitano, *Modern Quantum Mechanics*, 3rd ed. Cambridge University Press, 2020.

[16] A. D. Shapere, F. Wilczek, and Z. Xiong, "Models of Topology Change," *arXiv preprint*, 2012, [Online]. Available at: https://arxiv.org/abs/1210.3545

[17] U. Smilansky and G. Sofer, "Time evolution and the Schrödinger equation on time dependent quantum graphs," *Journal of Physics A: Mathematical and Theoretical*, vol. 57, no. 65204, 2024, doi: 10.1088/1751-8121/ad1fb6.

[18] D. A. Spielman, *Spectral and Algebraic Graph Theory*. Yale University, 2025. [Online]. Available at: http://cs-www.cs.yale.edu/homes/spielman/sagt

[19] N. Sprinkart, E. Scheer, and A. Di Bernardo, "Tutorial: From Topology to Hall Effects—Implications of Berry Phase Physics," *Journal of Low Temperature Physics*, vol. 217, pp. 686–719, 2024, doi: 10.1007/s10909-024-03219-6.

[20] Tanaka A. and Cheon T., "A topological formulation for exotic quantum holonomy," *Nanosystems: Physics, Chemistry, Mathematics*, vol. 6, no. 6, pp. 786–792, 2015, doi: https://doi.org/10.17586/2220-8054-2015-6-6-786-792.

[21] A. Tibbling, "New Studies of the Figure Eight Quantum Graph," Master's thesis, 2025. [Online]. Available at: https://urn.kb.se/resolve?urn=urn:nbn:se:kth:diva-361482

[22] V. Kostrykin and R. Schrader, "Kirchhoff's rule for quantum wires," *J. Phys. A: Math. Gen.*, vol. 32, no. 4, pp. 595–630, 1999, doi: 10.1088/0305-4470/32/4/006.

[23] V. Kostrykin and R. Schrader, "Kirchhoff's rule for quantum wires. II. The inverse problem with possible applications to quantum computers.," *Fortschr. Phys.*, vol. 48, no. 8, pp. 703–716, 2000, doi: 10.1002/1521-3978(200008)48:8703::AID-PROP7033.0.CO;2-O.

[24] J. A. Wheeler, "On the nature of quantum geometrodynamics," *Annals of Physics*, vol. 2, no. 6, pp. 604–614, 1957, doi: 10.1016/0003-4916(57)90050-7.